

**DYE SENSITIZED SOLAR CELL: PARAMETERS CALCULATION AND MODEL INTEGRATION****Ahmed. A. El Tayyan**

Physics Department, Al Azhar University, Gaza, Palestine

ahmedtayyan@yahoo.com

Received 2/11/2011., online 6/11/2011

Abstract-- This article proposes an accurate approach to calculate the internal parameters of a dye sensitized solar cell DSSC (L , α , m , D , n_0 , τ). This approach is based on the electron diffusion differential model and the values of the short circuit current density J_{sc} , the open circuit voltage V_{oc} , and the current density and the voltage at the maximum power point *i.e.* J_{mp} and V_{mp} , respectively.

Assuming, that the charge transfer at the counter electrode is potential controlled, the Butler-Volmer equation is adequately integrated with both the electron diffusion differential model, and the Schottky barrier model to account for the interfacial effect at counter electrode/electrolyte and TiO_2/TCO interfaces on the J-V characteristics. Some parametric analyses were conducted to study the effect of temperature, and electrode thickness on various DSSC parameters.

Keywords: DSSC, solar cell, photovoltaic

I. INTRODUCTION

In the last two decades, the dye sensitized solar cell (DSSC) has received much attention [1-8]. DSSCs have certain advantages over conventional silicon and thin film photovoltaic devices, due to the simplicity of the manufacturing process and the cost-effectiveness of most of the cell materials, which makes this type of solar cells feasible for mass production.

Currently, DSSC can achieve 11.1% energy conversion efficiency [9]. Further improvement is highly relied on better understanding of the energy conversion mechanisms and precise modeling for design optimization. In general, a DSSC comprises a nanocrystalline titanium dioxide (TiO_2) or zinc oxide (ZnO) electrode modified with a dye deposited on a transparent conducting oxide (TCO). A counter electrode is another TCO coated with a platinum (Pt) thin layer. An electrolyte solution with a dissolved iodide ion/triiodide ion redox couple (I^-/I_3^-) is added between the electrodes.

Efficient electron injection from excited dye to TiO_2 (or ZnO) plays an important role in DSSC [10,11].

The flow of the injected electrons through the porous TiO_2 film to the TCO depends on the incident intensity and trapping–detrapping effect [12]. Subsequently, the electrons flow to the counter electrode via an external load. The oxidized dye molecules are regenerated by redox mediators (I^-/I_3^-). Finally, for a complete DSSC operation cycle, the oxidized redox mediators (I_3^-) are transported to the counter electrode where regeneration of redox mediators occurs [13]. Due to the very small nanoparticle size (about 20nm) together with the strong screening effect of electrolyte, there is no significant macroscopic electric field in most of the porous thin films. Therefore, both electrons and redox mediators are transported mainly by diffusion.

The photoinjection of electrons from excited dye to TiO_2 conduction band increases the electron density in the porous electrode thin film, resulting in shifting the quasi-Fermi level E_F closer to the conduction band edge E_c . Theoretical models assume that the difference between E_F of TiO_2 and the electrolyte redox potential E_{redox} be the induced photovoltage [14-16]. That is true for the open-circuit condition in which there is no current flow through the TiO_2/TCO interface and electrolyte/counter electrode interface. However, under maximum power conditions, additional potential differences across these two interfaces should be considered.

This article describes a method to calculate the internal parameters of DSSC (L , α , m , D , n_0 , τ). This approach provides a tool for researchers to estimate theoretically the internal parameters instead of digging through literature for their experimental value. Also, the effect of voltage loss at the counter electrode/electrolyte interface on the total voltage and the behavior of the cell are theoretically investigated.

II. MODELING

Due to the wide spread in DSSC research, the scientific community is interested in experimentally and theoretically investigation of the photoelectrochemical behavior of nanostructured electrodes of DSSC. Södrgren *et al.* [14] has suggested a simple model which is basically based on two equations. The first one is a

continuity equation that describes the transport, recombination, and generation of electrons within the nanoporous film:

$$D \frac{\partial^2 n(x)}{\partial x^2} - \frac{n(x) - n_0}{\tau} + \Phi_0 \alpha \exp(-\alpha x) = \frac{\partial n}{\partial t} \quad (1)$$

where $n(x)$ is the excess concentration of the photogenerated electrons at position x within the film measured from the TiO₂/transparent conducting oxide (TCO) interface, n_0 is the concentration of electrons under equilibrium conditions in dark, τ is the conduction band free electrons life time, D is the diffusion coefficient of electrons, Φ_0 is the illumination intensity (incident photon flux, cm⁻² s⁻¹), and α is the light absorption coefficient of the porous film. Under a steady-state condition of an irradiated DSSC, Eq. (1) becomes

$$D \frac{\partial^2 n(x)}{\partial x^2} - \frac{n(x) - n_0}{\tau} + \Phi_0 \alpha \exp(-\alpha x) = 0. \quad (2)$$

The possibility of trapping-detrapping of electrons is not included in Eq. (2) since it is only important under nonsteady-state conditions [17]. Under short-circuit conditions, electrons are easily extracted as photocurrent and none of the electrons are drawn directly to the counter electrode. Therefore, the two boundary conditions are:

$$n(0) = n_0, \quad (3)$$

and

$$\left. \frac{dn}{dx} \right|_{x=d} = 0, \quad (4)$$

where d is the porous electrode thickness.

The second equation completing the model links the excess concentration of photogenerated electrons at the back contact, $n_{contact}$, with the photovoltage, V_{ph} , through the following expression [14, 18]

$$\left| V_{ph} \right| = \frac{kT}{q} m \ln \frac{n_{contact}}{n_0}, \quad (5)$$

where k is the Boltzmann constant, q is the elementary charge, T is the absolute temperature and m is an ideality factor. Equation (2) can be solved using the boundary conditions in Eq. (3), and Eq. (4). The short circuit current density J_{sc} can be obtained as [14, 18]:

$$J_{sc} = \frac{q\Phi L\alpha}{1 - L^2\alpha^2} \left[-L\alpha + \tanh\left(\frac{d}{L}\right) + \frac{L\alpha \exp(-d\alpha)}{\cosh\left(\frac{d}{L}\right)} \right], \quad (6)$$

where L is the electron diffusion length given by:

$$L = \sqrt{D\tau}. \quad (7)$$

If the DSSC operates under a potential difference V between the Fermi level of the TiO₂ and the redox

potential of the electrolyte, the density of the electrons at the TiO₂/TCO interface ($x = 0$) increases to n giving a new boundary condition:

$$n(0) = n. \quad (8)$$

The second boundary condition at $x = d$ remains unchanged as shown in Eq. (4). Solving Eq. (2) and using Eq. (5) yields the relationship between the current density and V [14,18] :

$$V = \frac{kTm}{q} \ln \left[\frac{L(J_{sc} - J)}{qDn_0 \tanh\left(\frac{d}{L}\right)} + 1 \right]. \quad (9)$$

This equation can be re-arranged to have the form:

$$J = J_{sc} - \frac{qDn_0}{L} \tanh\left(\frac{d}{L}\right) \left(\exp\left(\frac{qV}{kTm}\right) - 1 \right). \quad (10)$$

III. CALCULATING THE INTERNAL PARAMETERS OF DSSC

To determine the internal parameters of DSSC (Φ , L , α , m , D), one needs five pieces of information. These pieces of information are the short circuit current (J_{sc}) given by Eq. (6), open circuit voltage (V_{oc}), current and voltage at the maximum power point (J_{mp} and V_{mp}), respectively. The fourth and the fifth pieces of information required for the calculation of the five parameters can be obtained by realizing that the slope of the power at the maximum power point (dP/dV_{mp}) and (dP/dJ_{mp}) are equal to zero. Thus, at the open circuit voltage and at the maximum power point Eq.(9) becomes:

$$V_{oc} = \frac{kTm}{q} \ln \left[\frac{LJ_{sc}}{qDn_0 \tanh\left(\frac{d}{L}\right)} + 1 \right], \quad (11)$$

$$V_{mp} = \frac{kTm}{q} \ln \left[\frac{L(J_{sc} - J_{mp})}{qDn_0 \tanh\left(\frac{d}{L}\right)} + 1 \right]. \quad (12)$$

Additional two equations can be derived using the fact that on the P-V and P-J characteristics of a DSSC at the maximum power point, the derivatives of power with respect to voltage and with respect to current are equal to zero, that is;

$$\left(\frac{dP}{dV} \right)_{V=V_{mp}} = \frac{d(JV)}{dV} = J + \frac{dJ}{dV} V = 0. \quad (13)$$

$$J = J_{mp}$$

$$\left(\frac{dP}{dJ}\right)_V = V_{mp} = \frac{d(JV)}{dJ} = V + \frac{dV}{dJ} J = 0. \quad (14)$$

$$J = J_{mp}$$

The five internal parameters of DSSC (L , α , m , D , n_0) can be obtained by simultaneously solving Eq. (6), and Eq. (11) through Eq. (14) using the Mathcad solve block (Given Find) and by implementing the method of Conjugate Gradients. The value of the conduction band free electrons life time τ is obtained by substituting the values of the electron diffusion length L and the diffusion coefficient of electrons D into Eq. (7), then, the J-V characteristics can be generated using Eq. (6) and Eq. (9). Calculations were done using light intensity $\Phi = 1.0 \times 10^{17} \text{ cm}^{-2}\text{s}^{-1}$ which is equivalent to 1 sun condition (100 mW/cm^2) [15,18,19], temperature $T = 300 \text{ K}$, and porous layer thickness $d = 10 \times 10^{-4} \text{ cm}$.

The values of J_{sc} , V_{oc} , J_{mp} , and V_{mp} are determined from the JV characteristics obtained by substituting the published values of the parameters into Eq. (10) (see table 1). Then, the obtained values of J_{sc} , V_{oc} , J_{mp} , and V_{mp} are implemented into Eq. (6), and Eq.(11) through Eq. (14) to obtain the internal parameters of the DSSC, see Table I. Notice that the calculated values are of the same order as the published values.

TABLE I: A comparison between the calculated values and the published values of DSSC internal parameters.

Parameter	Published value	Calculated value
$L \text{ (cm}^{-1}\text{s}^{-1}\text{)}$	2.2361×10^{-3}	2.0747×10^{-3}
$\alpha \text{ (cm}^{-1}\text{)}$	5000 Refs. [15,18,19]	5138.9831
M	4.5 Refs. [15,18,19]	4.4662
$D \text{ (cm}^2\text{s}^{-1}\text{)}$	5.0×10^{-4} Ref [18]	3.9353×10^{-4}
N_0	10^{16} Refs[18,20,21]	1.2911×10^{16}
$\tau \text{ ms}$	10 Refs. [15,18,22]	10.9378

A good match between the current-voltage and the power-voltage characteristics obtained using the published values of the parameters [18], and the theoretically fitted current density-voltage and power-voltage curves obtained using the present method is illustrated in Fig. 1 and Fig. 2, respectively.

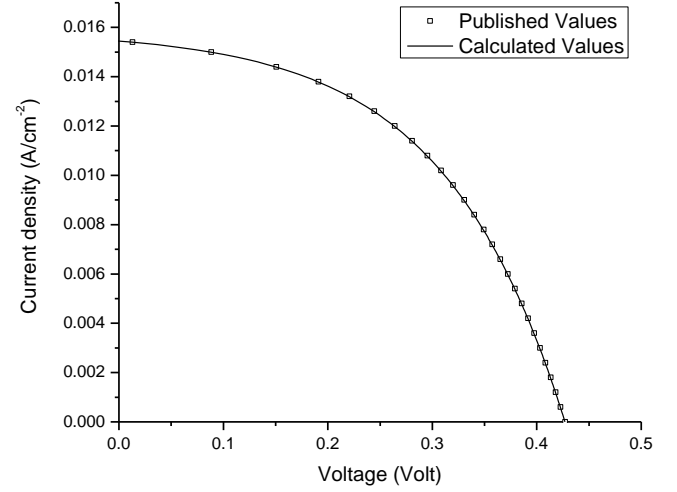


Fig.1: J-V Characteristics. Points are published data [18], line is calculated data.

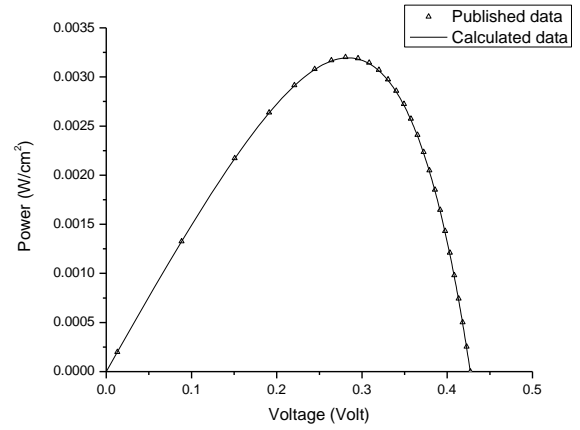


Fig. 2: Power-voltage characteristics. Points are published data [18]. Line is calculated data.

IV. INTEGRATING THE MODEL

Figure 3 illustrates the band energy levels of DSSC. In the dark, the potentials of TiO_2 , TCO, and the counter electrode are equal to the redox potential of the electrolyte as illustrated in Fig.3.a. Upon irradiation of the DSSC, the quasi-Fermi levels of TiO_2 are raised due to photoinjection as illustrated in Fig.3.b. Therefore the reference photovoltage can be expressed as:

$$V = V_0 - V_1 - V_2, \quad (15)$$

where V_0 is the potential difference between the TiO_2 Fermi level (E_F) and the redox potential of the electrolyte (E_{redox}). Here, V_0 represents the same voltage given in Eq. (9) and (10). On the other hand, V_1 is the voltage loss at

the TiO₂/TCO interface, and V₂ is the voltage loss at the counter electrode/electrolyte interface.

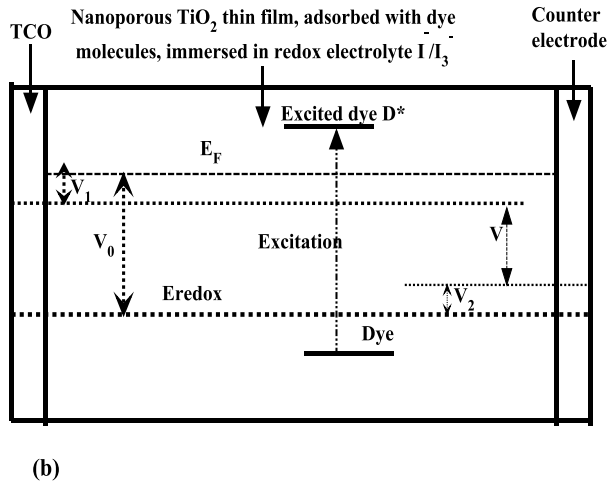
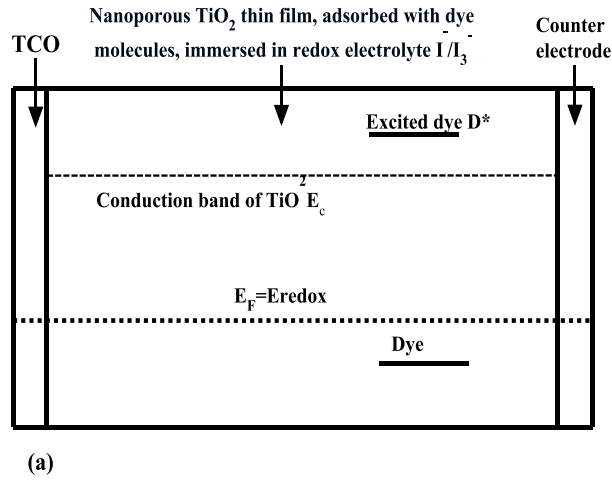


Fig. 3: Potential diagrams of DSSC: (a) in dark and (b) under illumination.

Meng *et al* [23] have suggested that highly doped and highly conductive TCO can be considered as a metal, and the TiO₂/TCO interface can be simulated by Schottky barrier model. Under illumination, the flow of electrons through the TiO₂/TCO interface causes a voltage loss V₁. This voltage loss can be correlated by the following expression referring to the thermionic emission theory:

$$J = A^* T^2 \exp\left(\frac{-q\phi_b}{kT}\right) \left[\exp\left(\frac{qV_1}{kT}\right) - 1 \right], \quad (16)$$

and

$$A^* = \frac{4\pi m^* q k^2}{h^3}, \quad (17)$$

where ϕ_b is Schottky barrier height; h is Planck's constant equal to $6.626 \times 10^{-34} \text{ m}^2 \text{ kg s}^{-1}$, m^* is equal to 5.6 times the free electron mass m_e for TiO₂, and A^* is Richardson's constant of TiO₂ equal to $6.71 \times 10^6 \text{ Am}^{-2} \text{ K}^{-2}$. Equation (16) can be rearranged to have the form:

$$V_1 = \frac{kT}{q} \ln \left[1 + \frac{J}{A^* T^2 \exp(-q\phi_b/kT)} \right]. \quad (18)$$

In order to find an expression for V₂, one needs to the following assumption that the charge transfer at the counter electrode is potential controlled, thus the current over the interface is independent of the concentrations of the redox ions at the interface. It is only dependent on the potential. Thus, the current can be described by the Butler-Volmer equation:

$$J = J_0 \left(\exp\left(\beta \frac{q}{kT} V_2\right) - \exp\left(- (1 - \beta) \frac{q}{kT} V_2\right) \right) \quad (19)$$

where J_0 is the exchange current density and β is a symmetry parameter with a value ranges between 0 and 1. A symmetry parameter of 0.5 describes a charge transfer reaction, which is symmetric forward and reverse potential. In this article we assume symmetric reaction $\beta = 0.5$.

Expanding the two exponentials in Eq.(19), taking into account, only, the first three terms of the expansion of each exponential and simplifying terms yields:

$$J = J_0 \frac{q}{kT} V_2, \quad (20)$$

or,

$$V_2 = \frac{kT}{J_0 q} J. \quad (21)$$

A charge transfer resistance R_{CT} of dimension $\Omega \text{ cm}^{-2}$ thus can be defined as shown in Eq. (22). The dimension of R_{CT} is the same as for a contact resistance.

$$\frac{1}{R_{CT}} = J_0 \frac{q}{kT}. \quad (22)$$

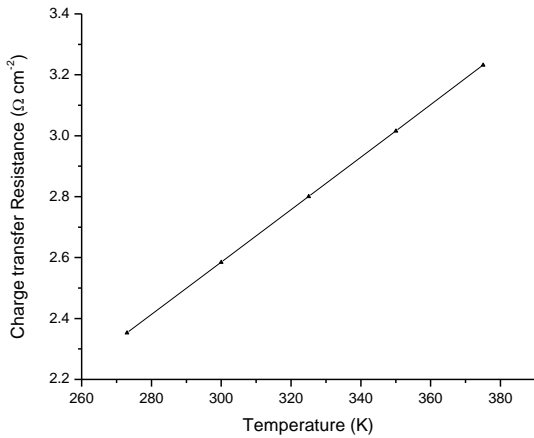


Fig. 4: The variation of the exchange resistance with temperature.

The back electrode of a DSSC is covered with some platinum, acting as a catalyst for the redox reaction. Provided the charge transfer resistance is not too high, it is a good approximation to describe electrolyte/platinized TCO contact by an ohmic charge transfer resistance and the Nernst equation [21]. A low R_{CT} corresponds to a high exchange current density, which is essential for a DSSC with good performance [21]. The variation of R_{CT} with temperature is illustrated in Fig. 4. The exchange resistance increases with increasing temperature.

The diffusion controlled charge transfer reaction is not considered in this article since it is effective at higher voltage. In contrast, a Butler Vollmerian behavior is observed at low voltages.

Meng *et al.* [23] showed that at the TiO_2/TCO interface there exists a critical value of ϕ_b , below which V_1 is negligible. At ϕ_b value higher than the critical value, V_1 increases with increasing ϕ_b . In this article, a value of ϕ_b equal to 0.5 eV which is below the critical value is chosen, in order to focus on the contribution of V_2 on the overall cell behavior.

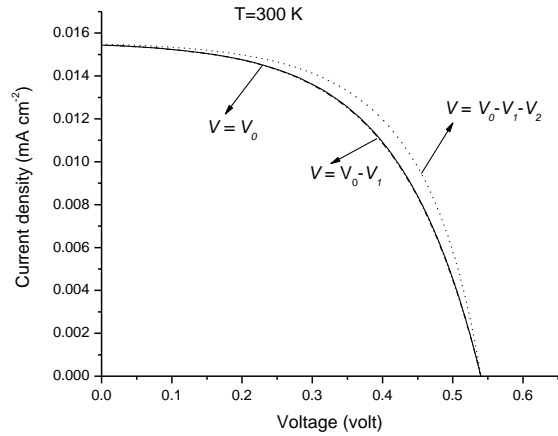


Fig. 5: A comparison between the theoretically calculated J-V characteristics showing the effect of including the voltages loss V_0 , V_0-V_1 , and $V_0-V_1-V_2$ at 300 K.

Figure 5 illustrates a comparison between the calculated J-V characteristics using Eq. (9), V_0 , and the effect of including the voltage loss at the TiO_2/TCO interface V_1 ; and the voltage loss V_2 at the counter electrode at 300 K. It is clear that inclusion of V_1 term doesn't affect the J-V characteristics. On the other hand, the inclusion of the V_2 term affects the maximum power point location, but it doesn't affect the short circuit current and the open circuit voltage points. The same behavior is found at higher temperature values. At lower temperature values, the inclusion of the voltage loss V_1 shows some deviation by lowering the maximum power point as shown in Fig 6.

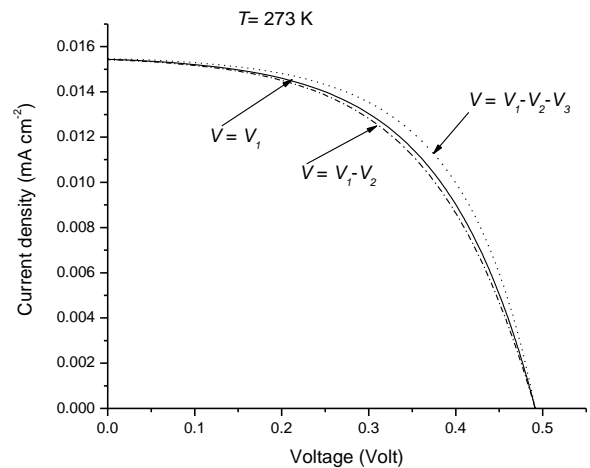


Fig. 6: A comparison between the theoretically calculated J-V characteristics showing the effect of including the voltages loss V_0 , V_0-V_1 , and $V_0-V_1-V_2$ at 273 K.

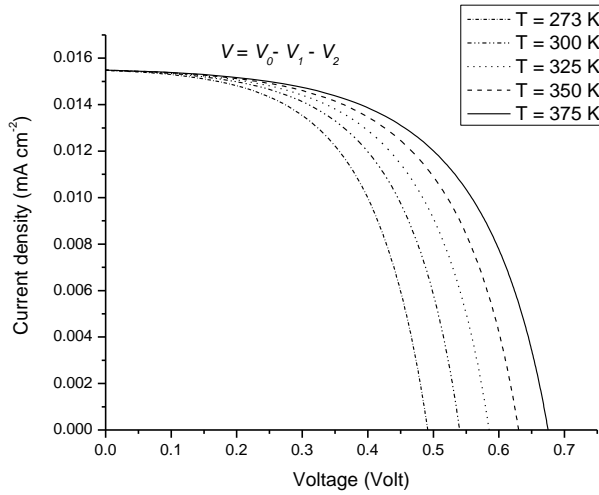


Fig.7: The calculated J-V characteristics at various temperatures.

The J-V characteristics at various temperature values are depicted in Fig.7. The open circuit voltage V_{oc} as well as the maximum power increase with increasing temperature, and the short circuit current J_{sc} is not affected as expected.

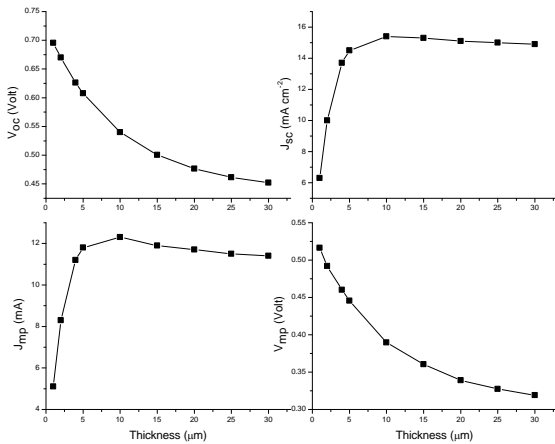


Fig. 8: The variations of V_{oc} , J_{sc} , J_{mp} , and V_{mp} with porous film thickness.

Figure 8 illustrates the variations of V_{oc} , J_{sc} , J_{mp} , and V_{mp} with porous film thickness. The results show that V_{oc} and V_{mp} decrease monotonically with increasing film thickness. This phenomenon can be explained by the electron dilution effect [15]. As light is transmitted through the porous electrode, the intensity gradually decreases. Therefore, as the thickness increases, the excessive electron density becomes lower resulting in a decrease in V_{oc} and V_{mp} . Also, a thicker electrode with a

higher series resistance contributes to the decrease in V_{oc} and V_{mp} [18].

The short circuit current and the maximum power current increase abruptly with increasing thickness as depicted in Fig. 8, then reach a peak, and decrease gradually afterward. The variations of J_{sc} and J_{mp} with thickness can be easily explained by electron photogeneration. For a given porosity and pore size, any increase in electrode thickness is directly increases the internal surface area of the semiconductor, resulting in a higher dye loading. Therefore, a thicker electrode can absorb more photons, leading to higher J_{sc} and higher J_{mp} . However, if the thickness of the electrode is greater than the penetration depth, the number of photons useful for photogeneration of electrons will reach a limit causing no further increase in J_{sc} and J_{mp} . Instead, an increase in the thickness beyond the light penetration depth yields more recombination centers that cause more electron loss and resulting in a gradual decrease in J_{sc} and J_{mp} .

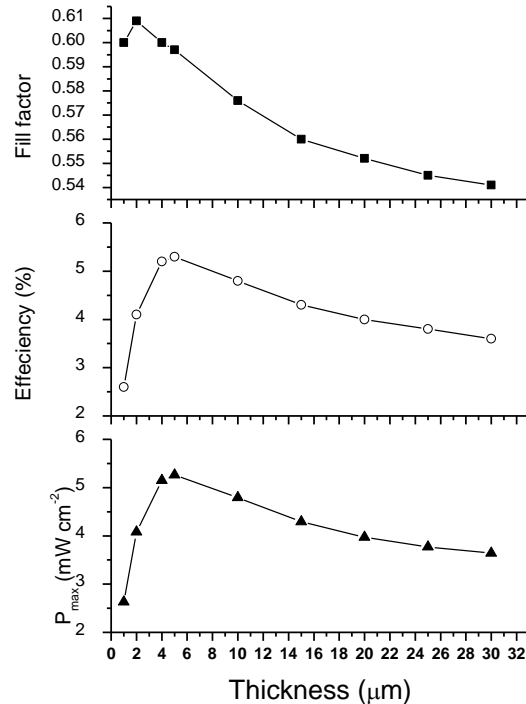


Fig. 9: The variations of fill factor, efficiency, and maximum power with electrode thickness.

The variations of fill factor, efficiency, and maximum power with electrode thickness is depicted in Fig. 9. The fill factor decreases with increasing electrode thickness, indicating an increase in the cell internal resistance. It is clear from the figure that the efficiency and the maximum power relation with thickness follow the same variation since the energy conversion efficiency of DSSC is the ratio of maximum output power to the incident light power. An optimal electrode thickness of

about 5 μm is inferred from Fig. 9 which is consistent with the theoretical finding of Ming. *et al* [18].

V. COMPARISON WITH PUBLISHED EXPERIMENTAL DATA

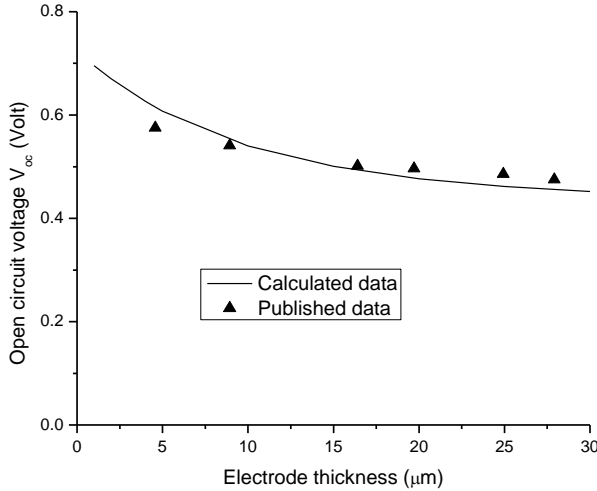


Fig. 10: Comparison between the calculated data and published experimental data from ref. [24] of V_{oc} vs. electrode thickness for $\Phi=1.0 \times 10^{17} \text{cm}^{-2} \text{s}^{-1}$, $\alpha=5000 \text{cm}^{-1}$, $D=5.0 \times 10^{-4} \text{cm}^2 \text{s}^{-1}$, $m=4.5$, and $\tau=10 \text{ms}$.

Although much work on DSSC has been published in literature, studies of the effect of electrode thickness are limited. In this section some relevant previous experimental work are presented for comparison with the modeling results of this investigation. Mercurochrome sensitized solar cells have been studied by Hara *et al.* [24] who investigated the effect of different photoelectrode materials, *i.e.* TiO_2 , Nb_2O_5 , ZnO , SnO_2 , and In_2O_3 . They found that as the thickness of TiO_2 increased from 4.5 to 28 μm , the V_{oc} decreased from 0.58 to 0.48 V. The predicted V_{oc} by the current investigation agreed well with Hara *et al.* experimental data as shown in Fig. 10.

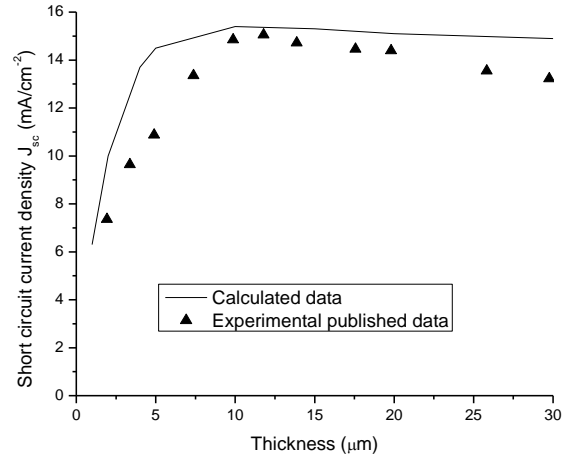


Fig. 11: Comparison between the calculated data and published experimental data from ref. [25] of J_{sc} vs. electrode thickness for $\Phi=1.0 \times 10^{17} \text{cm}^{-2} \text{s}^{-1}$, $\alpha=5000 \text{cm}^{-1}$, $D=5.0 \times 10^{-4} \text{cm}^2 \text{s}^{-1}$, $m=4.5$, and $\tau=10 \text{ms}$.

Fukai *et al* [25] have experimentally investigated the variation of J_{sc} with photoelectrode thickness using SnO_2 as photoelectrode and using N719 dye as photon absorber. Figure 11 shows that the present modeling is consistent with the experimental work of Fukai *et al* [25] which shows that the measured J_{sc} increases significantly with electrode thickness and reaches the maximum at an electrode thickness of about 11 μm . Further increase in photoelectrode thickness would cause a slight decrease in J_{sc} .

The different values of optimal electrode thickness found by individual research groups may be attributed to different dye molecules of various light absorption coefficients. The microstructure parameters, such as TiO_2 particle size, pore size, porosity, and roughness factor, have significant effects on the electron diffusion coefficient, electron life time, light absorption coefficient, as well as specific surface area, resulting in apparent difference in the DSSC performance [26-29]. Thus it is important to model the performance of a DSSC with respect to the microstructure of its photoelectrode [26,29].

VI. CONCLUSIONS

An accurate approach to calculate the internal parameters of a DSSC (L , α , m , D , n_0 , τ) is proposed in this article. This method provides a tool for researchers to estimate theoretically the internal parameters instead of digging through literature for their experimental value. This approach is based on the electron diffusion differential model and the values of the short circuit current density J_{sc} , open circuit voltage V_{oc} , and the

current density and voltage at the maximum power point *i.e.* J_{mp} and V_{mp} , respectively. By assuming that the charge transfer at the counter electrode is potential controlled, the Butler-Volmer equation is integrated with the electron diffusion differential model, and the Schottky barrier model to account for the interfacial effect at counter electrode/electrolyte and TiO₂/TCO interfaces on the J-V characteristics. Parametric analyses were conducted to study the effect of temperature, and electrode thickness on various cell parameters.

References

[1] B. M. O'Regan, and M. Grätzel, M., "A low-cost, high-efficiency solar cell based on dye-sensitized colloidal TiO₂ films", *Nature*, **353**, 737-740 (1991).
 [2] F. T. Kong, S. Y. Dai, and K. T. Wang, "New Amphiphilic Polypyridyl Ruthenium(II) Sensitizer and Its Application in Dye-Sensitized Solar Cells", *Sol. Energy Mater. Sol. Cells*, **25**, 168-171 (2007).
 [3] G. Smestad, C. Bignozzi, and R. Argazzi, "Testing of dye sensitized TiO₂ solar cells I: Experimental photocurrent output and conversion efficiencies", *Sol. Energy Mater. Sol. Cells*, **32**, 259-272 (1994).
 [4] G. Smestad, "Testing of dye sensitized TiO₂ solar cells II: Theoretical voltage output and photoluminescence efficiencies", *Sol. Energy Mater. Sol. Cells*, **32**, 273-288 (1994).
 [5] A. Kay, and M. Grätzel, "Low cost photovoltaic modules based on dye sensitized nanocrystalline titanium dioxide and carbon powder", *Solar Energy Mater. Solar Cells*, **44**, 99-117 (1996).
 [6] S. Y. Dai, J. Weng, Y. F. Sui, C. W. Shi, Y. Huang, S. H. Chen, X. Pan, X. Q. Fang, L. H. Hu, F. T. Kong, and K. J. Wang, "Dye-Sensitized Solar Cells, from Cell to Module", *Sol. Energy Mater. Sol. Cells*, **84**, 125-133, (2004).
 [7] J. Halme, M. Toivola, A. Tolvanen, and P. Lund, "Charge transfer resistance of spray deposited and compressed counter electrodes for dye-sensitized nanoparticle solar cells on plastic substrates", *Solar Energy Materials & Solar Cells*, **90**, 872-886 (2006).
 [8] J. Xia, N. Masaki, M. Lira-Cantu, Y. Kim, K. Jiang, and S. Yanagida, "Influence of Doped Anions on Poly(3,4-ethylenedioxythiophene) as Hole Conductors for Iodine-Free Solid-State Dye-Sensitized Solar Cells", *J. Am. Chem. Soc.*, **130**, 1258-1263 (2008).
 [9] Y. Chiba, A. Islam, Y. Watanabe, R. Komiya, N. Koide, and L. Han., "Dye-Sensitized Solar Cell with Conversion Efficiency of 11.1%" *Japanese Journal of Applied Physics*, **45**, 638-640 (2006).
 [10] G. Franco, J. Gehring, L. M. Peter, E. A. Ponomarev, and I. Uhlendorf, "Frequency-Resolved Optical Detection of Photoinjected Electrons in Dye-Sensitized Nanocrystalline Photovoltaic Cells", *J. Phys. Chem. B*, **103**, 692-698, (1999).

[11] N. J. Cherepy, G. P. Smestad, M. Grätzel, J. Z. and Zhang, "Ultrafast Electron Injection: Implications for a Photoelectrochemical Cell Utilizing an Anthocyanin Dye-Sensitized TiO₂ Nanocrystalline Electrode", *J. Phys. Chem. B*, **101**, 9342-9351, (1997).
 [13] K. Imoto, K. Takahashi, T. Yamaguchi, T. Komura, J. Nakamura, and K. Murata, "High-performance carbon counter electrode for dye-sensitized solar cells", *Sol. Energy Mater. Sol. Cells*, **79**, 459-469 (2003).
 [14] S. Södergren, A. Hagfeldt, J. Olsson, and S. E. Lindquist., "Theoretical Models for the Action Spectrum and the Current-Voltage Characteristics of Microporous Semiconductor-Films in Photoelectrochemical Cells", *J. Phys. Chem.*, **98**, 5552-5556 (1994).
 [15] R. Gómez, and P. Salvador, "Photovoltage Dependence on Film Thickness and Type of Illumination in Nanoporous Thin Film Electrodes According to a Simple Diffusion Model", *Solar Energy Materials & Solar Cells*, **88**, 377-388 (2005).
 [16] J. Ferber, R. Stangl, and J. Luther, "An electrical model of the dye-sensitized solar cell", *Sol. Energy Mater. Sol. Cells*, **53**, 29-54 (1998).
 [17] J. Nelson, in: A.J. Bard, M. Stratmann (Eds.), *Encyclopedia of Electrochemistry*, (Wiley-VCH, Weinheim, **6**, 432 (2002).
 [18] N. Meng, M. K. H. Leung, and D. Y. C. Leung, "Theoretical Modelling of the Electrode Thickness on Maximum Power Point of Dye-Sensitized Solar Cell", *The Canadian Journal of Chemical Engineering*, **86**, 35-42 (2008).
 [19] J. J. Lee, G. M. Coia, and N. S. Lewis, "Current Density Versus Potential Characteristics of Dye-Sensitized Nanostructured Semiconductor Photoelectrodes. 2. Simulation", *J. Phys. Chem. B*, **108**, 5282-5293 (2004).
 [20] G. Rothenberger, D. Fitzmaurice, and M. Grätzel, "Optical Electrochemistry. 3. Spectroscopy of Conduction-Band Electrons in Transparent Metal-Oxide Semiconductor-Films-Optical Determination of the Flat-Band Potential of Colloidal Titanium-Dioxide Films", *J. Phys. Chem.*, **96**, 5983-5986 (1992).
 [21] J. Ferber, and J. Luther, "Modeling of Photovoltage and Photocurrent in Dye-Sensitized Titanium Dioxide Solar Cells", *J. Phys. Chem. B*, **105**, 4895-4903 (2001).
 [22] L. Dloczik, O. Ileperuma, I. Lauermann, L. M. Peter, E. A. Ponomarev, G. Redmond, N. J. Shaw, and I. Uhlendorf, "Dynamic Response of Dye-Sensitized Nanocrystalline Solar Cells: Characterization by Intensity Modulated Photocurrent Spectroscopy", *J. Phys. Chem. B*, **101**, 10281-10289 (1997).
 [23] N. Meng, M. K. H. Leung, D. Y. C. Leung, and K. Sumathy, "Theoretical modeling of TiO₂/TCO interfacial effect on dye-sensitized solar cell performance", *Solar Energy Materials & Solar Cells*, **90**, 2000-2009 (2006).

- [24] K. Hara, T. Horiguchi, T. Kinoshita, K. Sayama, H. Sugihara, and H. Arakawa, "Highly Efficient Photon-to-Electron Conversion with Mercurochrome-Sensitized Nanoporous Oxide Semiconductor Solar Cells", *Sol. Energy Mater. Sol. Cells*, **64**, 115-134 (2000).
- [25] Y. Fukai, Y. Kondo, S. Mori, and E. Suzuki, "Highly Efficient Dye-Sensitized SnO₂ Solar Cells having Sufficient Electron Diffusion Length", *Electrochem. Commun.*, **9**, 1439-1443 (2007).
- [26] N. G. Park, G. Schlichthorl, J. Van de Lagemaat, H. M. Cheong, A. Mascarenhas, and A. J. Frank., "Dye-Sensitized TiO₂ Solar Cells: Structural and Photoelectrochemical Characterization of Nanocrystalline Electrodes Formed from the Hydrolysis of TiCl₄", *J. Phys. Chem. B*, **103**, 3308-3314 (1999).
- [27] J. van de Lagemaat, K. D. Benkstein, and A. J. Frank: "Relation between Particle Coordination Number and Porosity in Nanoparticle Films, "Implications to Dye-Sensitized Solar Cells", *J. Phys. Chem. B*, **105**, 12433-12436, (2001).
- [28] M. J. Cass, A. B. Walker, D. Martinez, and L. M. Peter, "Grain Morphology and Trapping Effects on Electron Transport in Dye-Sensitized Nanocrystalline Solar Cells", *J. Phys. Chem. B*, **109**, 5100-5107 (2005).
- [29] S. Nakade, Y. Saito, W. Kubo, T. Kitamura, Y. Wada, and S. Yanagida., "Influence of TiO₂ Nanoparticle Size on Electron Diffusion and Recombination in Dye-Sensitized TiO₂ Solar Cells ", *J. Phys. Chem. B*, **107**, 8607-8611, (2004).